# Direct Power Control Method of Maximum Power Point Tracking (MPPT) Algorithm for Pico-Hydrokinetic River Energy Conversion System

W.I. Ibrahim[1[0000-0002-9572-1913]], M. R. Mohamed [1[0000-0002-9194-0553]] and R. M. T. R. Ismail [2[0000-0002-2146-1450]]

[1] Sustainable Energy & Power Electronics Research Group,
[2] Instrumentation & Control Engineering (ICE),
Faculty of Electrical & Electronics Engineering
Universiti Malaysia Pahang
26600 Pekan, Pahang, MALAYSIA.
wismail@ump.edu.my

**Abstract.** In this paper, a design of maximum power point tracking (MPPT) algorithm for the pico-hydrokinetic system in river application has been proposed. The design topology consists of the permanent magnet synchronous generator (PMSG), a three-phase bridge rectifier and a DC boost converter. The proposed MPPT algorithm is a combination of modified hill-climbing search algorithm (MHCS) with the current PI-controller. The MPPT concept is based on measuring the rectifier output voltage and current respectively to produce the reference current ($I_{MPP}$). The PI-controller has been used to tune the error signal between $I_{MPP}$ and actual inductance current ($I_{dc}$) to provide the duty-cycle of the boost converter. A comparison is performed between the fixed step HCS and the proposed MPPT to investigate the performance of the algorithm. The results show the proposed algorithm able to harness the maximum power with 96.32% efficiency.

**Keywords:** MPPT, Hill Climbing Search Algorithm, Hydrokinetic.

## 1 Introduction

The use of renewable energy as a clean and sustainable energy resource is rapidly increasing every year and expected to keep growing worldwide. This is due to the exhaustion of fossil fuels and the environmental concern such as the emission of $CO_2$ and greenhouse effect [1]. Instead of solar PV, wind energy, biomass and geothermal, the pico-hydrokinetics also has been explored for future energy resources.

The pico-hydrokinetic system has many advantages such as the system generate the electricity without requires any dam or other structures and give minimal impacted to the environment [2]. This type of energy harnessing can be applied at the rivers, man-made waterway and other flowing facilities with an optimal water velocity[3].

The maximum power point tracking (MPPT) algorithm can be implemented to the pico-hydrokinetic system to extract more power by keeping the optimum steady

voltage across the load. In addition, the fluctuation of water velocity in a river is a challenging issue especially to design the control system that able to harness the maximum output power with high efficiency.

The MPPT algorithm from the wind energy conversion system (WECS) and solar PV has been adopted in this study to be implemented in the pico-hydrokinetic system. This is due to the concepts of operation, electrical hardware and variable speed generator are similar to WECS [4]. Therefore, the MPPT algorithm from WECS is the primary reference for details research in this field.

The MPPT algorithm can be categorised into three groups in general, an indirect power control (IPC), a direct power control (DPC) and soft-computing method (SCM) as shown in Fig. 1. The IPC MPPT is based on maximising the mechanical power ($P_m$) while DPC MPPT algorithm directly maximised the output power ($P_o$) [5].

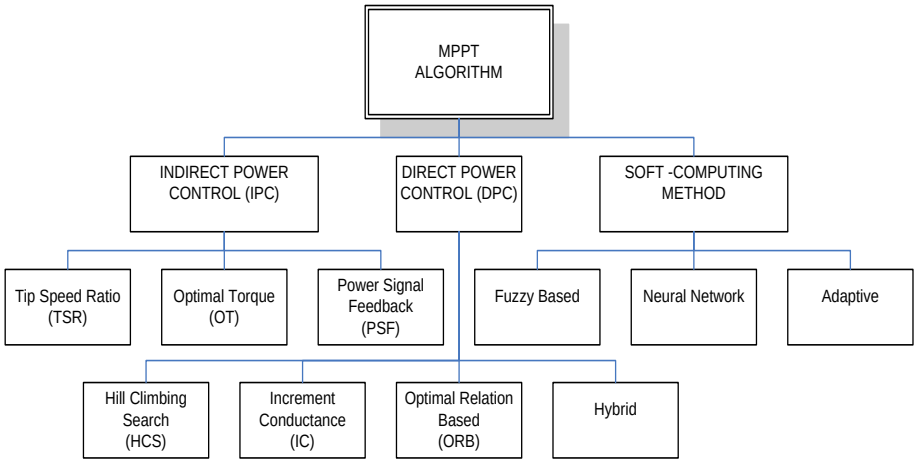


**Fig. 1**. The MPPT Algorithm classification

The IPC based MPPT algorithm such as the tip speed ratio (TSR) and optimal torque(OT) are commonly used for large wind turbine system. The system algorithm requires the sensor to measure the wind speed and both rotational speed of turbine and generator.In [6] the quantum neural network (QNN) has been used as a controller to enhance the efficiency of TSR and OT MPPT method in the WECS.

The DPC MPPT algorithm is suitable for small scale wind turbine system. This algorithm is also a sensorless method and not required turbine parameters knowledge in designing the control algorithm. Hence, this type of algorithm is more reliable and less complex with a lower cost[7]. The perturb & observe (P&O) and also known as hill-climbing search (HCS) are broadly used because of the flexible and straightforward algorithm [8]. In [9], the variable-step HCS has been proposed to solve the wrong direction tracking of conventional HCS algorithm.

Several MPPT algorithms using soft computing method have been proposed in [10]–[13]. The methods are promising with higher efficiency and excellent performance under varying wind speed conditions. However, the algorithm is very sophisticated and the convergences speed is low due to the quantity of iteration and

training knowledge in the programming. In reference [14] the online step and offline step are required to train the different set of neural network parameters for the optimal neural network controller. Hence, the trained neural network can quickly map the relationship between input and output data.

In this paper, direct power control based MPPT algorithm for the pico-hydrokinetic system has been designed to harness the maximum power in the variation of water. The design topology consists of PMSG, uncontrolled rectifier and DC boost converter as a control circuit. The modified hill-climbing search algorithm with the current PI controller has been proposed to enhance the capturing of maximum output power and efficiency of the system.

## 2 Pico-Hydrokinetic System Configuration

Figure 2 shows the circuit topology of the pico-hydrokinetic system used in this studied. The water turbine is directly coupled to the permanent magnet synchronous generator (PMSG). A three-phase uncontrolled rectifier is used to rectify the generator output voltage. The DC Boost converter is used to perform the MPPT operation by controlling the IGBT switching. By using this circuit topology, the system required only one active power switch. This method will reduce the cost and simplified the control of the hydrokinetic system. Also, the resistance (*R*) is directly connected to the output of the boost converter as a load to consume the energy of the system. However, this topology can be substituted by the power inverter for a grid-connected and stand-alone operation.

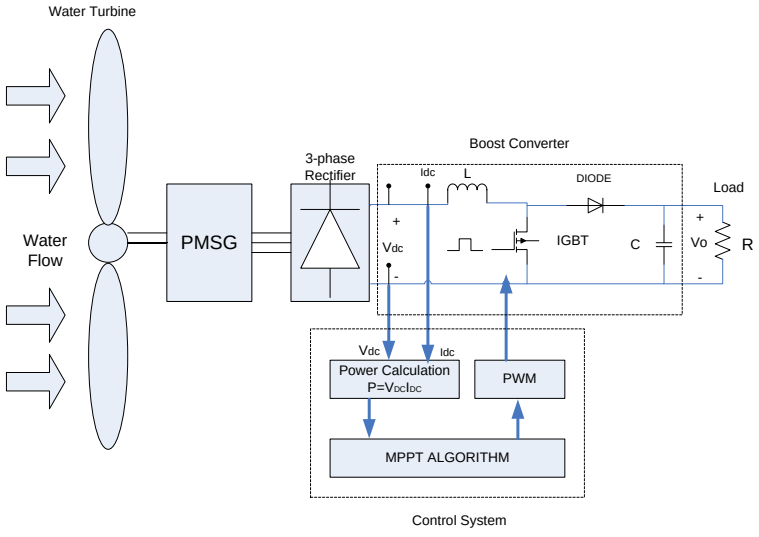


**Fig.2**. Circuit topology understudied

## 2.1 Turbine Model

Water velocity is an input of the pico-hydrokinetic while the output is the mechanical power ($P_m$) and torque developed ($T_m$) to drive the generator shaft. The amount of power that could be harnessing in the river is given by

$$P_m = \frac{1}{2}\rho A V^3 C_p \quad (1)$$

where, $\rho$ is water density (1000 Kg/m$^3$), $A$ is the cross-sectional area of the turbine (m$^2$), $V$ is the water current velocity (m/s) and $C_p$ is the power coefficient of the turbine. The pitch angle (β) is fixed for the water turbine. Hence, the $C_p$ is merely a function of the tip speed ratio ($\lambda$) which is the ratio of the linear speed of the blade to the water current velocity.

$$TSR(\lambda) = \frac{\omega R}{V} \quad (2)$$

where, the $\omega$ is the rotational speed of the turbine and $R$ is the turbine radius. The turbine characteristic indicates that there is one specific *TSR* value which turbines are working at the most efficient operating point. Thus, the *TSR* value should be kept at an optimal operating point for all water current velocity to achieve the maximum energy harnessing.

The turbines power coefficient ($C_p$) is determined by the *TSR*, shape and radius of the turbines [15]. The relationship between $C_p$ and *TSR* used in this paper is expressed as;

$$C_P(\lambda) = -0.022\lambda^6 + 0.04\lambda^5 - 0.26\lambda^4 + 0.72\lambda^3 - 0.77\lambda^2 + 0.27\lambda - 0.011 \quad (3)$$

The turbine mechanical torque ($T_m$) can be given by;

$$T_m = \frac{P_m}{\omega_m} \quad (4)$$

where $P_m$ is the mechanical power and $\omega_m$ is the turbine rotational speed. Fig. 3 shows the modelling of the hydrokinetic turbine based on the derivation of Eq. (1)-(4). It is observed that the power produced by the turbine depends on the value of the water density ($\rho$), the swept area ($A$), power coefficient ($C_p$ )and input water velocity ($V$).

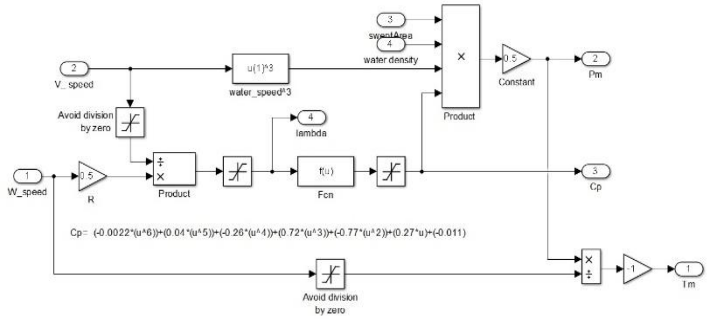


**Fig. 3**. Pico-hydrokinetic turbine model

## 2.2 Analysis of PMSG and Rectifier

The PMSG has been used to convert the turbine rotational speed into electrical power. The back electromotive force (E) of the PMSG with constant flux is given by,

$$E = k\omega_m \quad (5)$$

where K is a constant coefficient and $\omega_m$ is the generator rotor speed (rad/s). The terminal phase voltage in a balanced steady state is given by

$$V_s = E - I_s\left(R_s + j\omega_e L_s\right) \quad (6)$$

where $I_s$, $R_s$ and $L_s$ is the stator current, stator resistance, and stator inductance respectively. Whereas, $\omega_e$ is the electrical frequency. The relationship between the electrical frequency ($\omega_e$) and the mechanical frequency ($\omega_m$) is given by;

$$\omega_e = p\omega_m \quad (7)$$

where $p$ is the number of PMSG poles. The function of the bridge rectifier to convert the generated AC voltage from PMSG to a DC voltage. The relationship between the DC Voltage ($V_{DC}$) and a phase AC voltage of PMSG ($V_s$) can be expressed as;

$$V_{DC} = \frac{3\sqrt{6}}{\pi} V_S \quad (8)$$

The approximate relationship between $V_{DC}$ and $\omega_m$ can be expressed from (5)-(8) [16]

$$V_{DC} \approx \omega_m \quad (9)$$

The considering the output power conversion from PMSG into DC power through the rectification process is at unity power factor with no losses, the output power ($P_g$) can be expressed as [17];

$$P_g = 3V_s I_s = V_{DC} I_{DC} \quad (10)$$

## 2.3 Design of DC Boost Converter

The DC Boost converter is commonly used because of the high efficiency in power transfer. However, the energy can be transfer when the output stage voltage is higher than the input voltage [18]. The output voltage of the boost converter can be controlled by varying the duty cycle. Fig. 3 shows the equivalent circuit of the DC boost converter with insulated gate bipolar switch (IGBT) used as a power switch (S). By varying the duty cycle ($D$), the load seen by the generator will be changing. Thus, the output voltage and rotational rotor speed will be adjusted accordingly [19].

The ratio between the output voltage ($V_{out}$) to the input voltage $V_{DC}$ is given by;

$$\frac{V_{out}}{V_{DC}} = \frac{1}{1-D} \quad (11)$$

where, $D$ is the duty cycle and $V_{DC}$ is the output voltage from rectifier or input voltage to boost converter.

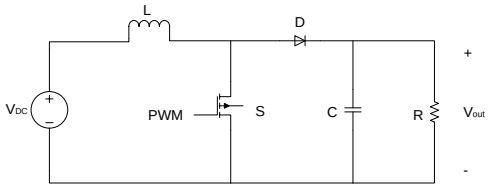


**Fig. 4**. DC boost converter equivalent circuit

In continuous conduction mode (CCM) operation, the value of inductor and capacitor can be given;

$$L = \frac{V_{DC} D}{2\Delta I_L f_s} \tag{12}$$

where $\Delta I_L$ is the desired inductor current peak ripple and *fs* is the boost converter switching frequency. The value of the capacitor (C) can be determined by:

$$C = \frac{V_{out} D}{2\Delta_{vo} R f_s} \tag{13}$$

where $\Delta_{vo}$ is the output voltage peak ripple and *R* is the resistance load. Table 1 shows the parameter design of boost converter used in this studied.

**Table 1.** The parameter of the boost converter.

| Parameter | Values |
|---|---|
| Input Capacitor, $C_{in}$ (μF) | 100 |
| Output Capacitor, $C_{out}$ (μF) | 245 |
| Inductance, L (mH) | 1.85 |
| Load Resistance $R_{Load}$ (Ω) | 10.0 |
| Switching Frequency, $f_s$ (kHz) | 20 |

# 3 MPPT Control Algorithm

## 3.1 Hill-Climbing Search Algorithm

Hill-climbing search (HCS) algorithm will locate the local maximum point by climbing the curve by adding the fixed step size (ΔS). The HCS algorithm is based on perturb and observe (P&O) concept that used to climb the power curve of the turbine. The algorithm will monitor any changes in the output power and rotational rotor speed with respect to water velocity. The maximum power $P_{MPP}$ can be generated from the PMSG when the variation of power over the variation of rotor speed equal to zero as shown in Fig.5.

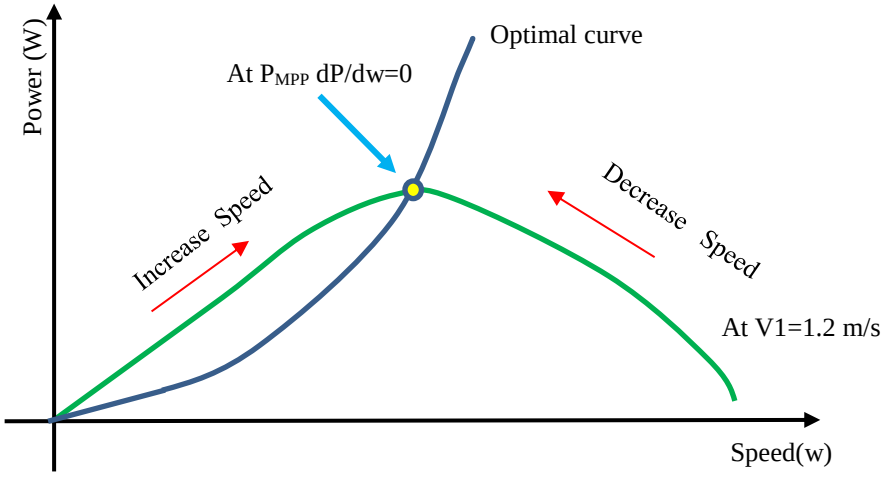


**Fig. 5**. HCS Concept based on the regulation of the duty cycle

The flow-chart of HCS MPPT algorithm was shown in Fig. 6. In this approach, if the operating point is at the left region of the peak point ($P_{MPP}$), the controller must move it to the right by climbing the curve to the nearest peak point. The step size (ΔS) must be added and the generator must increase the speed to achieve the $P_{MPP}$. In another side, if the operating point is in the right region of the peak point (PMPP), the controller must move to the left by reducing the step size (ΔS). Therefore, the generator must reduce the speed to achieve the $P_{MPP}$.

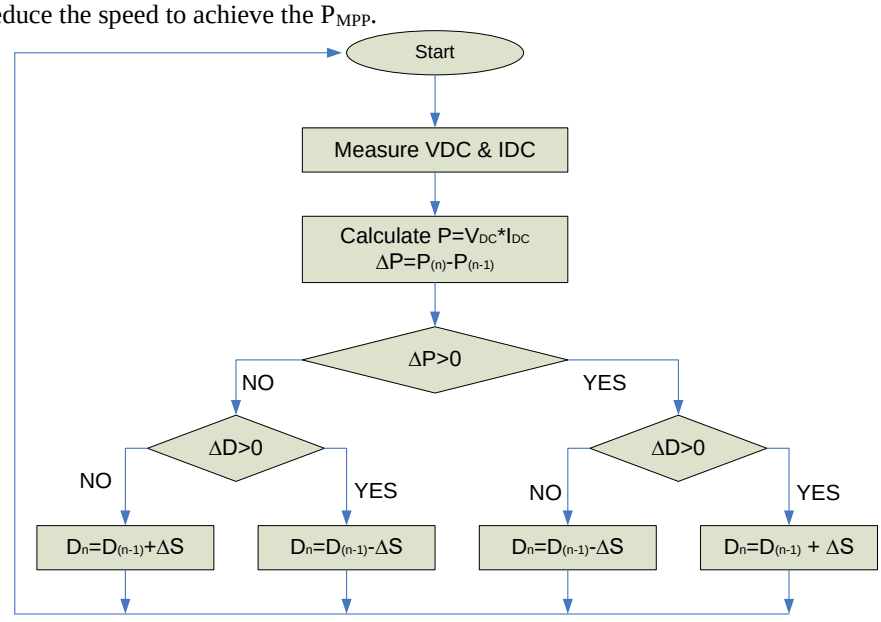


**Fig. 6**. HCS MPPT Algorithm

### 3.2 Proposes Modify Hill-Climbing Search with PI current Controller

The modified HCS algorithm will improve the fixed step HCS algorithm by reducing the oscillation at the steady-state condition. The simpler way to modify the algorithm is by changing the step-size (ΔI) as shown in Fig. 7. The ΔI is multiple by a constant value in ordered to provide the very responsive algorithm with maximum energy harnessing.

The following step describes the modified HCS algorithm with PI controller

Step 1: Measure the $V_{DC}$ and $I_{DC}$

Step 2: Calculate the power and change in electrical power ΔP

Step 3: Calculate the change in electrical voltage ΔV

Step 4: Determine the direction of the perturbation & observe the optimal operating condition

Step 5: Increment or decrement the $I_{MPP}$ and step size (ΔI) according to the formula as given;

$$I_{MPP} = I_{MPP(n-1)} \pm \Delta I \qquad 14$$

If the operating point at the left of $P_{MPP}$, increase the (ΔI) by multiple by 1. Otherwise, reduce the step size by multiple by 2.

Step 6: Updated the next actual value of P, V and $I_{MPP}$ for the next sample time.

Step 7: Calculate the error between $I_{MPP}$ and Idc and fed into PI-Controller.

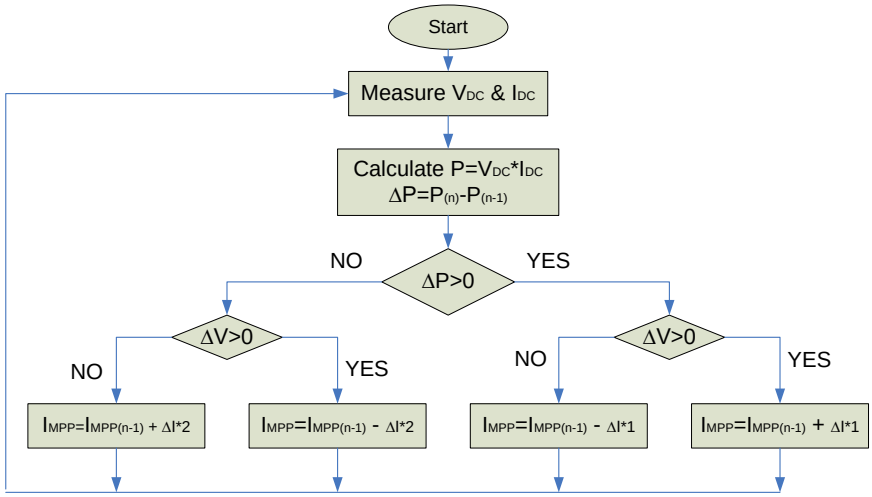


**Fig. 7**. Modified hill climbing search algorithm

The comparison between the actual current ($I_{DC}$) and reference current ($I_{MPP}$) to produce an error signal as shown in Fig.8. Then, the error signal is fed into the PI-controller for the tuning process. The output signal is compared to the repetitive triangular frequency waveform to generate the PWM for switching the DC Boost converter.

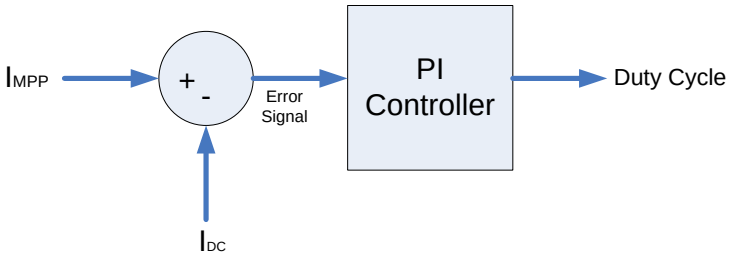


**Fig.8**. PI-controller block diagram

## 4 Results & Discussion

The Matlab/Simulink environment is used to perform the simulation study of the pico-hydrokinetic system in the river. Two performance indicators for the MPPT algorithm has been investigated in this study. First is the tracking ability of the algorithm and the second is the ability to capture the maximum output power at the fluctuation of water. Fig. 9 shows the complete system of the pico-hydrokinetic system with MHCS-PI controller.

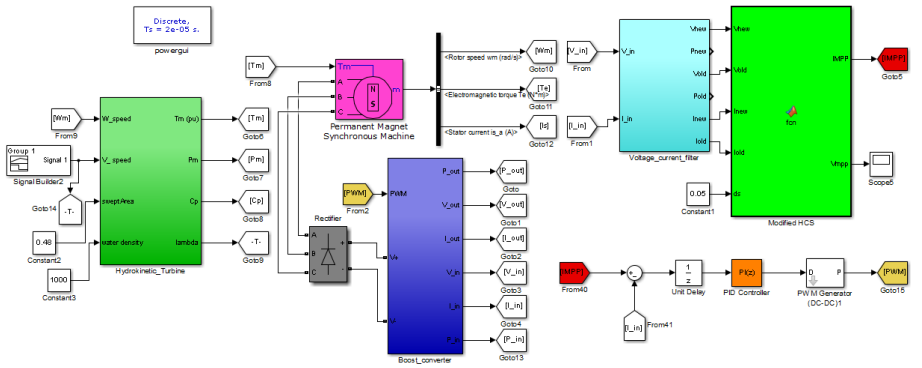


**Fig. 9.** The pico-hydrokinetic system with MPPT algorithm.

The input water velocity is varied from 0.5ms$^{-1}$ to 2.0ms$^{-1}$ as shown in Fig. 10 to investigate the tracking ability of the MPPT techniques

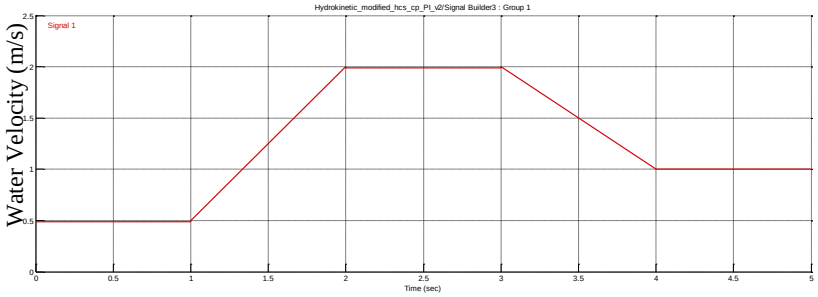


**Fig. 10**. The input water velocity

Figure 11 shows the tracking ability of both algorithms. As can be seen both algorithm able to track the variation of the input water velocity for optimal energy harnessing. Also, the Modified HCS-PI algorithm able to harness more output power than the HCS algorithm even at the fluctuation of water.

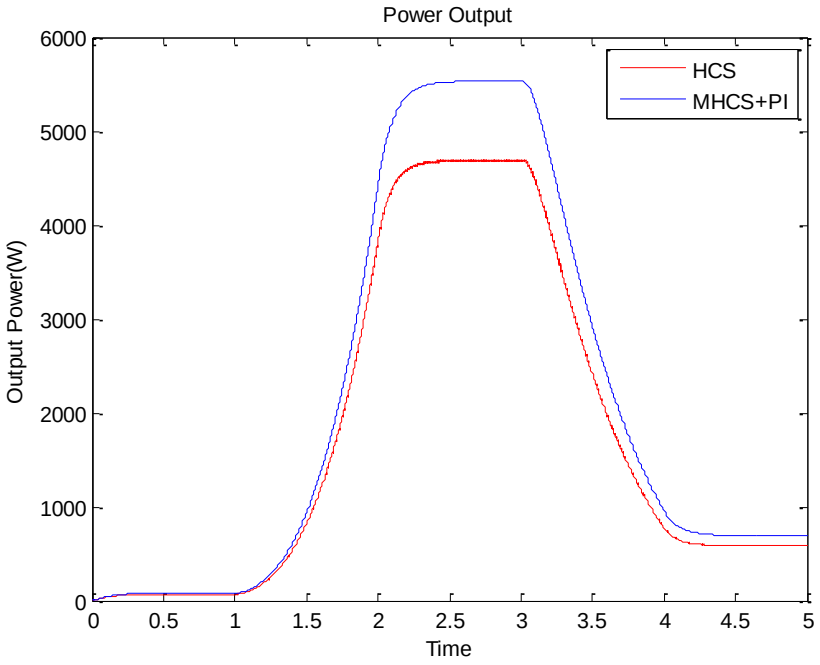


**Fig. 11**. The output powers.

Table 2 shows the performance comparison of HCS and MHCS-PI algorithm base MPPT controller. Both algorithms have been tested at fixed water velocity starting from 0.4 $ms^{-1}$ up to 2.0 $ms^{-1}$ to investigate total power generated and the efficiency of the algorithm. As can be seen, the MHCS-PI algorithm shows outstanding performance compared to the HCS algorithm. The MHCS-PI algorithm can harness the maximum power between 43.7 W to 5617W with average efficiency at 96.32%. However, the HCS algorithm only gains 81.66% efficiency with output power between 37.34 W to 4756 W.

**Table 2.** The comparison output power and efficiency of the MPPT algorithm.

| Water Velocity (m/s) | Theoretical (W) | Output Power (W) | | Efficiency (%) | |
|---|---|---|---|---|---|
| | | HCS | MHCS+PI | HCS | MHCS+PI |
| 0.4 | 46.08 | 37.3 | 43.7 | 81.0 | 94.8 |
| 0.8 | 368.64 | 299.2 | 353.4 | 81.1 | 95.8 |
| 1.2 | 1244.16 | 1016.0 | 1201.0 | 81.6 | 96.5 |
| 1.6 | 2949.12 | 2421.0 | 2862.0 | 82.0 | 97.0 |
| 2.0 | 5760.00 | 4756.0 | 5617.0 | 82.6 | 97.5 |

## 5 Conclusion

In this paper, the design topology for the pico-hydrokinetic system is presented. The proposed design consists of PMSG, uncontrolled rectifier, and DC boost converter. The HCS and MHCS-PI algorithm has been simulated to track the maximum power in different water velocity. The advantages of the proposed system have not required any sensors to measure the water velocity and operation of variable speed PMSG. Besides, the knowledge of turbines parameters and characteristics also not essentials in the proposed design. The results show that the pico-hydrokinetic system can harness between 43.7 W to 5617 W with 96.32 % efficiency by MHCS-PI algorithm.

## 6 Acknowledgement

The authors would like to thank to Universiti Malaysia Pahang for funding support under UMP Postgraduate Research Scheme (PGRS190318).

## References

[1] İ. Yazici and E. K. Yaylaci, "Maximum power point tracking for the permanent magnet synchronous generator-based WECS by using the discrete-time integral sliding mode controller with a chattering-free reaching law," *IET Power Electron.*, pp. 1751–1758, 2017.

[2] E. Alvarez Alvarez, M. Rico-Secades, E. L. Corominas, N. Huerta-Medina, and J. Soler Guitart, "Design and control strategies for a modular hydroKinetic smart grid," *Int. J. Electr. Power Energy Syst.*, vol. 95, pp. 137–145, 2018.

[3] M. I. Yuce and A. Muratoglu, "Hydrokinetic energy conversion systems: A technology status review," *Renew. Sustain. Energy Rev.*, vol. 43, pp. 72–82, 2015.

[4] S. P. Koko, K. Kusakana, and H. J. Vermaak, "Optimal energy management of a grid-connected micro-hydrokinetic with pumped hydro storage system," *J. Energy Storage*, vol. 14, pp. 8–15, 2017.

[5] D. Kumar and K. Chatterjee, "A review of conventional and advanced MPPT algorithms for wind energy systems," *Renew. Sustain. Energy Rev.*, vol. 55, pp. 957–970, 2016.

[6] S. Ganjefar, A. A. Ghassemi, and M. M. Ahmadi, "Improving efficiency of two-type maximum power point tracking methods of tip-speed ratio and optimum torque in wind turbine system using a quantum neural network," *Energy*, vol. 67, pp. 444–453, 2014.

[7] Z. M. Dalala, Z. U. Zahid, W. Yu, Y. Cho, and J. S. Lai, “Design and analysis of an MPPT technique for small-scale wind energy conversion systems,” *IEEE Trans. Energy Convers.*, vol. 28, no. 3, pp. 756–767, 2013.

[8] S. M. Raza Kazmi, H. Goto, H.-J. Guo, and O. Ichinokura, “A Novel Algorithm for Fast and Efficient Speed-Sensorless Maximum Power Point Tracking in Wind Energy Conversion Systems,” *Ind. Electron. IEEE Trans.*, vol. 58, no. 1, pp. 29–36, 2011.

[9] H. H. H. Mousa, A. Youssef, and E. E. M. Mohamed, “Electrical Power and Energy Systems Variable step size P & O MPPT algorithm for optimal power extraction of multi-phase PMSG based wind generation system,” *Electr. Power Energy Syst.*, vol. 108, no. December 2018, pp. 218–231, 2019.

[10] C. M. Hong, C. H. Chen, and C. S. Tu, “Maximum power point tracking-based control algorithm for PMSG wind generation system without mechanical sensors,” *Energy Convers. Manag.*, vol. 69, pp. 58–67, 2013.

[11] M. A. Abdullah, T. Al-Hadhrami, C. W. Tan, and A. H. M. Yatim, “Towards Green Energy for Smart Cities: Particle Swarm Optimization Based MPPT Approach,” *IEEE Access*, vol. 6, pp. 1–1, 2018.

[12] K. Kumar, R. N. Babu, and K. R. Prabhu, “Design and analysis of RBFN-based single MPPT controller for hybrid solar and wind energy system,” *IEEE Access*, vol. 5, no. August, pp. 15308–15317, 2017.

[13] S. Li, H. Wang, Y. Tian, and A. Aitouche, “A RBF neural network based MPPT method for variable speed wind turbine system,” *IFAC-PapersOnLine*, vol. 28, no. 21, pp. 244–250, 2015.

[14] S. Messalti, A. Harrag, and A. Loukriz, “A new variable step size neural networks MPPT controller: Review, simulation and hardware implementation,” *Renew. Sustain. Energy Rev.*, vol. 68, no. August 2015, pp. 221–233, 2017.

[15] R. Tiwari and N. R. Babu, “Fuzzy logic based MPPT for permanent magnet synchronous generator in wind energy conversion system,” *Int. Fed. Autom. Control*, vol. 49, no. 1, pp. 462–467, 2016.

[16] Y. Xia, K. H. Ahmed, and B. W. Williams, “A New Maximum Power Point Tracking Technique for Permanent Magnet Synchronous Generator Based Wind Energy Conversion System,” *IEEE Trans. Power Electron.*, vol. 26, no. 12, pp. 3609–3620, 2011.

[17] J. Hussain, “Adaptive Maximum Power Point Tracking Control Algorithm for Wind Energy Conversion Systems,” *IEEE Trans. ENERGY CONVERSION, VOL. 31, NO. 2, JUNE 2016*, vol. 31, no. 2, pp. 697–705, 2016.

[18] J. L. Daniel Zammit, Cyril Spiteri Staines, Alexander Micallef, Maurice Apap, “Incremental Current Based MPPT for a PMSG Micro Wind Turbine in a Grid-Connected DC Microgrid,” *Energy Procedia*, vol. 142, pp. 2284–2294, 2017.

[19] M. A. Abdullah, A. H. M. Yatim, C. W. Tan, and R. Saidur, “A review of maximum power point tracking algorithms for wind energy systems,” *Renew. Sustain. Energy Rev.*, vol. 16, no. 5, pp. 3220–3227, 2012.